









Complexation of Alkali and Alkaline Earth Metal Cations by Fluorescent Glycoconjugated Calix[4]arene Derivative: Thermodynamic and Computational Studies

 Matija Modrušan,¹  Nikola Cindro,^{1,*}  Andrea Usenik,¹  Katarina Leko,¹ Lucija Glazer,¹  Renato Tomaš,²
 Gordan Horvat,¹  Josip Požar,¹ and  Vladislav Tomišić^{1,*}

¹ Department of Chemistry, Faculty of Science, University of Zagreb, Horvatovac 102a, 10000 Zagreb, Croatia

² Division of Chemistry, Faculty of Chemistry and Technology, University of Split, Ruđera Boškovića 35, 21000 Split, Croatia

* Corresponding authors' e-mail address: ncindro@chem.pmf.hr, vtomisc@chem.pmf.hr

RECEIVED: July 15, 2024 * REVISED: September 23, 2024 * ACCEPTED: October 1, 2024

THIS PAPER IS DEDICATED TO THE LATE PROFESSOR TOMISLAV CVITAŠ

Abstract: The affinity of novel, phenanthridine-based calix[4]arene glycoconjugate (**L**), bearing efficient cation-binding tertiary-amide functionalities in the coordination site, towards alkali and alkaline earth metal cations in methanol was investigated by means of spectrophotometry, microcalorimetry, and ¹H NMR spectroscopy. Significant complexation-induced enhancement of the calixarene fluorescence was observed in all cases, allowing also the use of spectrofluorimetric titrations for quantitative monitoring of the complexation processes. The thermodynamic reaction parameters (complex stability constants, standard reaction enthalpies and entropies) were determined and discussed regarding the ligand structure and cation charge densities, as well as solvation effect on the studied equilibria. Compound **L** was found to be a considerably more efficient receptor for alkali relative to alkaline earth metal cations of similar sizes. This was mostly a consequence of stronger solvation of the latter compared to the former in methanol. Molecular dynamic simulations of **L** and its complexes were carried out as well, which provided additional information on their structural characteristics and the ligand cation-complexation properties.

Keywords: calixarenes, cation complexation, solvent effect, inclusion, fluorescence, thermodynamics, glycoconjugation.

INTRODUCTION

CALIXARENES are a class of supramolecular hosts that have been widely functionalized at their upper and/or lower rims, resulting in an array of exceptionally versatile compounds. Over the past several decades they have received great attention as ionophores and molecular receptors.^[1–6] Due to their structural diversity, various calixarene derivatives have been used as catalysts,^[7,8] ion extractants,^[6,9–13] surfactants,^[14,15] as well as electrochemical^[16,17] and fluorescent sensors.^[18–22] They also have significant potential in biochemical and medicinal applications, including their use as biomimetics,^[23–29] drug delivery systems,^[30,31] and ion channels.^[32,33]

Functionalization of calixarenes at the lower rim with electron-donating functionalities, such as those comprising carbonyl groups (amides, esters, ketones), considerably enhances their cation-binding capabilities.^[6,10,34–40] Among these, tertiary-amide-functionalized calixarenes form the most stable complexes due to the high basicity of the amide carbonyl oxygen, whereas the stability of complexes involving ester and ketone derivatives, as well as secondary amides, is significantly lower. The latter is mostly due to the intramolecular hydrogen bonds between amide groups which need to be disrupted upon cation binding.^[37,39,41–44]

Incorporating fluorescent groups into calixarene structures significantly increases their receptor sensitivity, allowing for the fluorimetric detection and quantitative

analysis of various analytes at significantly lower concentrations compared to the other spectrometric techniques often used.^[18,20,21,45–49] In our recent work, we have synthesized fluorescent tertiary-amide and ester calixarene derivatives, also bearing phenanthridine groups, and thoroughly investigated the equilibria of their reactions with alkali metal cations in various organic solvents.^[50] The possibility of cation coordination with phenanthridine nitrogen atoms was explored, and particular attention was paid to the inclusion of solvent molecule into the hydrophobic *basket* of free and complexed ligands, since this process was proven to have considerable allosteric influence on the extent of the cation-binding reactions.^[37,39,40,44,51–55] Most calixarene derivatives, especially those functionalized with bulky and usually non-polar moieties, are virtually water insoluble, or their solubility is scarce. This hinders their potential use in aqueous media, which is of great significance for various medicinal and biological applications. Numerous attempts have been made to enhance the solubility of calixarenes in water, commonly involving the incorporation of charged (e.g. sulfonyl^[56–59]) or hydrophilic polymeric groups (e.g. PEG^[60]). The former can cause interference with the ion binding due to the presence of counterions, whereas the latter often leads to formation of emulsions,^[60] limiting the possibility of their practical applications. Thus, the potential of calixarenes as cation receptors and sensors in aqueous solutions has remained a challenge. Dealing with this issue, we have published the synthesis of neutral calixarene derivatives containing amide functionalities with solubilizing glucose groups linked through triazole subunits, as well as detailed physicochemical investigations of their cation-binding equilibria.^[61] These ligands exhibited outstanding aqueous solubility ($> 0.01 \text{ mol dm}^{-3}$), and the affinity of the tertiary-amide-derivative possessing 8 glucose moieties towards Na^+ in water ($\log K = 5.15$) and methanol ($\log K = 7.24$) was substantial.^[61,62]

Encouraged by the above findings, we have envisioned analogous receptors additionally functionalized with fluorescent subunits with the aim of their utilization in various above-mentioned areas. The introduction of glucose-containing groups was expected to enhance the hydrophilicity of calixarenes, thereby increasing their solubility in polar solvents, like water and methanol. Hence, in this work we have synthesized calixarene derivative **L** (Scheme 1) that comprises tertiary-amide triazole-glucose functionalities together with highly fluorescent phenanthridine subunits, which can serve both as fluorophores and for ion coordination through their nitrogen atoms. Unfortunately, due to the presence of the latter bulky, hydrophobic groups, solubility of **L** in water was insufficient to allow for physicochemical investigations of its cation-binding in aqueous solution. Therefore, methanol was

chosen as the most water-like solvent for the studies of alkali and alkaline earth metal cations binding, which were carried out by means of spectrophotometry, spectrofluorimetry, microcalorimetry, and ^1H NMR spectroscopy. Our objectives were to investigate the thermodynamics governing the complexation equilibria and to get an insight into the cation-binding induced changes in the ligand fluorescence. Furthermore, molecular dynamics simulations were employed to explore the structural properties of **L** and its complexes, as well as the process of solvent molecule inclusion into their hydrophobic cavities.

EXPERIMENTAL

Materials

All reagents used for synthesis were *p.a.* grade, purchased from Aldrich, Merck, Ajelis, Kemika, Acros, and Alfa Aesar, and were used without further purification. Solvents were also *p.a.* grade and used without further purification except for acetone and dichloromethane which were purchased as technical grade and were distilled and dried under molecular sieves prior to use. Compound **P1**,^[47] 6-(chloromethyl)phenanthridine,^[63] *N,N*-bis(2-azidoethyl)-2-bromoacetamide,^[64,65] and propargyl-2,3,4,6-tetra-*O*-acetyl- β -D-glucopyranoside^[64,66] were prepared according to the previously published procedures, modified as described in the Supporting Information.

Cation solutions for complexation studies were prepared by weighing and dissolving the following salts: lithium perchlorate (Sigma Aldrich, 99.99%), sodium perchlorate (Fluka, 98+ %), potassium perchlorate (Fluka, 99+ %), rubidium chloride (Sigma Aldrich, ≥ 99.8 %), cesium chloride (Merck, 99.5 %), magnesium perchlorate hexahydrate (Sigma Aldrich, 99 %), calcium perchlorate tetrahydrate (Sigma Aldrich, 99 %), strontium perchlorate trihydrate (Alfa Aesar, 98 %), and barium perchlorate (Fluka, 98+ %) in previously distilled methanol (J. T. Baker, HPLC Gradient Grade).

Synthesis

Synthesis of 5,11,17,23-tetra-tert-butyl-25,27-bis((phenanthridin-6-yl)methoxy)-26,28-di(N,N-di(2-azidoethyl)aminocarbonylmethoxy)calix[4]arene (P2)

Compound **P1** (1.5 g, 1.4 mmol), *N,N*-bis(2-azidoethyl)-2-bromoacetamide (1.6 g, 5.8 mmol), and potassium carbonate (3.2 g, 23.0 mmol) were suspended in 21 mL of dry acetone. The suspension was refluxed with stirring for 3 days at 70 °C followed by cooling to room temperature after which DCM (100 mL) was added. The solution was washed with H_2O ($3 \times 50 \text{ mL}$), and the aqueous layer was extracted with DCM (50 mL). The organic layers were combined, and DCM was evaporated. The crude solid was dissolved in small amount of DCM and propan-2-ol was

added. The product precipitated after removal of DCM and it was filtered yielding 1.1 g (35 %) of pure **P2**.

¹H NMR (400 MHz, CDCl₃-d₁) δ / ppm: 8.66 (d, *J* = 8.27 Hz, 2H), 8.61 (dd, *J* = 8.35 Hz, 1.17 Hz, 2H), 8.20 (d, *J* = 8.13 Hz, 2H), 8.16 (dd, *J* = 8.05 Hz, 1.24 Hz, 2H), 7.83 (dt, *J* = 7.76 Hz, 0.81 Hz, 2H), 7.76 (dt, *J* = 7.54 Hz, 1.32 Hz, 2H), 7.70 (dt, *J* = 7.47 Hz, 1.54 Hz, 2H), 7.52 (dt, *J* = 7.76 Hz, 0.73 Hz, 2H), 7.00 (s, 4H), 6.43 (s, 4H), 5.60 (s, 4H), 4.77 (s, 4H), 4.64 (d, *J* = 12.89 Hz, 4H), 2.23 (s, 8H), 3.04 (d, *J* = 12.99 Hz, 4H), 2.93 (t, *J* = 5.87 Hz, 4H), 2.77 (t, *J* = 5.86 Hz, 4H), 1.28 (s, 18H), 0.86 (s, 18H); **¹³C NMR** (101 MHz, CDCl₃-d₁) δ / ppm: 170.1, 157.8, 153.6, 153.0, 145.1, 144.6, 143.7, 135.0, 133.0, 131.7, 130.6, 130.1, 128.8, 127.3, 125.9, 125.3, 124.8, 124.3, 122.1, 122.0, 77.2, 69.4, 50.0, 49.3, 47.3, 46.2, 34.0, 33.6, 32.2, 31.6, 31.2; **ATR-IR** (cm⁻¹) 2956, 2903, 2869, 2093, 1676, 1479, 1463, 1410, 1360, 1301, 1256, 1235, 1194, 1129, 1109, 1062, 1010, 989, 947, 871, 784, 761, 727, 697, 632, 615, 580, 556, 527, 506, 459, 419. **HRMS** (MALDI-TOF): *m/z* [M + Na]⁺; calculated for (C₈₄H₉₂N₁₆NaO₆) 1443.7283; found 1443.7299.

Synthesis of 5,11,17,23-tetra-tert-butyl-25,27-bis((phenanthridin-6-yl)methoxy)-26,28-di(N,N-bis(2-(4-(((2R,3R,4S,5S,6R)-3,4,5-triacetyloxy-6-(acetyloxymethyl)tetrahydro-2H-pyran-2-yl)oxy)methyl)-1H-1,2,3-triazol-1-yl)ethyl)aminocarbonylmethoxy)calix[4]arene (P3)

Compound **P2** (500 mg, 0.35 mmol) was dissolved in 25 mL of DCM with sodium perchlorate (171 mg, 1.4 mmol). After one hour of stirring, propargyl-2,3,4,6-tetra-*O*-acetyl-β-D-glucopyranoside (544 g, 1.4 mmol), CuI (28 mg, 0.15 mmol), DIPEA (26 μL, 0.15 mmol), and AcOH (8.4 μL, 0.15 mmol) were added. The mixture was stirred for 3 days at room temperature after which DCM was added to a total of 200 mL, and washed with ammonia solution (50 mL, V(H₂O):V(25 % NH₃) = 3:1) and mQ H₂O (10 × 100 mL). The organic layer was filtered through cotton wool and the solvent was evaporated. The crude solid was dissolved in small amount of DCM and *n*-hexane was added. After removal of DCM, the product started to crystallize to give 660 mg (63 %) of analytically pure **P3**.

¹H NMR (400 MHz, CDCl₃-d₁) δ / ppm: 8.62 (d, *J* = 8.30 Hz, 2H), 8.55 (d, *J* = 7.98 Hz, 2H), 8.04 (d, *J* = 8.30 Hz, 2H), 7.97 (d, *J* = 8.30 Hz, 2H), 7.81 (t, *J* = 7.66 Hz, 2H), 7.68 (qt, *J* = 5.75 Hz, 4H), 7.49 (t, *J* = 7.66 Hz, 2H), 7.39 (s, 2H), 7.20 (s, 2H), 7.01 (s, 4H), 6.40 (s, 4H), 5.63 (q, *J* = 7.34 Hz, 4H), 5.17 (q, *J* = 9.44 Hz, 4H), 5.08 (q, *J* = 9.44 Hz, 4H), 4.98 (q, *J* = 9.44 Hz, 4H), 4.93–4.49 (m, 20H), 4.32–4.09 (m, 12H), 3.85 (t, *J* = 5.93 Hz, 4H), 3.72 (t, *J* = 6.20 Hz, 4H), 3.26 (q, *J* = 6.20 Hz, 8H), 2.97 (t, *J* = 11.87 Hz, 4H), 2.05 (s, 12H), 2.02 (s, 12H), 1.98 (s, 12H), 1.93 (s, 12H), 1.25 (s, 18H), 0.84 (s, 18H); **¹³C NMR** (151 MHz, CDCl₃-d₁) δ / ppm: 170.6, 170.2, 169.4, 169.4, 157.8, 153.4, 153.2, 145.6, 144.9, 143.9, 143.9,

143.5, 135.1, 135.0, 132.8, 131.5, 131.5, 130.9, 129.7, 129.0, 127.5, 127.4, 127.0, 126.1, 126.1, 125.2, 124.8, 124.8, 124.2, 123.8, 123.7, 122.4, 122.2, 100.0, 99.9, 72.8, 72.8, 71.9, 71.9, 71.2, 69.5, 68.3, 64.4, 62.7, 61.8, 61.8, 48.7, 48.3, 47.7, 47.4, 34.0, 33.7, 32.1, 32.1, 31.6, 31.1, 31.1, 25.4, 20.8, 20.7, 20.6; **ATR-IR** (cm⁻¹) 2958, 2909, 2869, 1749, 1658, 1480, 1365, 1218, 1125, 1037, 909, 872, 764, 731, 598, 488. **HRMS** (MALDI-TOF): *m/z* [M + H]⁺; calculated for (C₁₅₂H₁₈₁N₁₆O₄₆) 2967.2349; found 2967.2502.

Synthesis of 5,11,17,23-tetra-tert-butyl-25,27-bis((phenanthridin-6-yl)methoxy)-26,28-di(N,N-bis(2-(4-(((2R,3R,4S,5S,6R)-3,4,5-trihydroxy-6-(hydroxymethyl)tetrahydro-2H-pyran-2-yl)oxy)methyl)-1H-1,2,3-triazol-1-yl)ethyl)aminocarbonylmethoxy)calix[4]arene (L)

Compound **P3** was dissolved in 15 mL of MeOH after which, while stirring, 15 mL of saturated NH₃ in MeOH was added. The mixture was stirred for 24 h at room temperature followed by evaporation of solvent. The crude solid was dissolved in MeOH (20 mL), and diethyl ether (80 mL) was added with vigorous stirring. The precipitated product was filtered to give 330 mg (78 %) of pure compound **L**.

¹H NMR (600 MHz, CDCl₃-d₁) δ / ppm: 8.73 (d, *J* = 8.51 Hz, 2H), 8.66 (d, *J* = 8.15 Hz, 2H), 8.39 (d, *J* = 8.15 Hz, 2H), 8.02 (d, *J* = 8.15 Hz, 2H), 7.89 (t, *J* = 8.51 Hz, 2H), 7.89 (s, 2H), 7.73 (t, *J* = 7.09 Hz, 2H), 7.70 (t, *J* = 7.09 Hz, 2H), 7.66 (s, 2H), 7.64 (t, *J* = 7.45 Hz, 2H), 7.00 (s, 4H), 6.49 (s, 4H), 5.67 (q, *J* = 7.45 Hz, 4H), 4.96 (d, *J* = 12.41 Hz, 2H), 4.85 (d, *J* = 12.41 Hz, 2H), 4.76 (d, *J* = 12.41 Hz, 2H), 4.69 (s, 4H), 4.65 (d, *J* = 12.76 Hz, 4H), 4.48 (dd, *J* = 13.52 Hz, 8.26 Hz, 4H), 4.43 (d, *J* = 7.80 Hz, 2H), 4.37 (d, *J* = 12.41 Hz, 2H), 4.33 (t, *J* = 6.38 Hz, 4H), 3.95 (t, *J* = 6.03 Hz, 4H), 3.91 (d, *J* = 12.05 Hz, 4H), 3.69 (dd, *J* = 12.05 Hz, 5.32 Hz, 6H), 3.45 (t, *J* = 5.67 Hz, 4H), 3.39 (q, *J* = 8.15 Hz, 6H), 3.32–3.22 (m, 10H), 2.95 (dd, *J* = 13.12 Hz, 6.03 Hz, 4H), 1.22 (s, 18H), 0.89 (s, 18H); **¹³C NMR** (151 MHz, CDCl₃-d₁) δ / ppm: 170.8, 157.8, 153.3, 153.2, 145.2, 144.5, 142.9, 134.8, 133.0, 132.0, 131.1, 129.0, 128.9, 127.5, 127.5, 127.4, 125.8, 125.2, 124.7, 124.6, 124.5, 124.4, 124.3, 122.3, 122.2, 102.4, 102.2, 76.7, 76.6, 76.3, 73.6, 73.6, 70.2, 70.2, 69.8, 61.7, 61.5, 61.4, 61.4, 33.5, 33.3, 31.7, 30.7, 30.5, 30.4, 23.9; **ATR-IR** (cm⁻¹) 3353, 2957, 2909, 2875, 1654, 1481, 1460, 1362, 1305, 1236, 1193, 1076, 1038, 871, 764, 731, 631, 580. **HRMS** (MALDI-TOF): *m/z* [M + H]⁺; calculated for (C₁₂₀H₁₄₉N₁₆O₃₀) 2295.0659; found 2295.0688.

Other details on the synthetic procedures and characterization of compounds are given in Supporting Information.

Physicochemical Measurements

Spectrophotometric titrations were performed using Agilent Cary 60 spectrophotometer. Titrations were conducted by stepwise addition of metal salt solution

($c_0 = 1 \times 10^{-3} \text{ mol dm}^{-3}$ to 0.1 mol dm^{-3}) into the thermostatted (25.0 ± 0.1) °C quartz cuvette (Hellma, Suprasil QX, $l = 1 \text{ cm}$) containing ligand solution ($c_0 = 8 \times 10^{-5} \text{ mol dm}^{-3}$ to $1 \times 10^{-4} \text{ mol dm}^{-3}$). Spectra were recorded with baseline correction at 1 nm data interval and an integration time of 0.2 s. The obtained spectrophotometric data were processed by HypSpec program.^[67]

Spectrofluorimetric experiments were carried out by means of Agilent Cary Eclipse spectrofluorimeter. Titrations were conducted by stepwise addition of metal salt solution ($c_0 = 1 \times 10^{-3} \text{ mol dm}^{-3}$ to $2 \times 10^{-2} \text{ mol dm}^{-3}$) into the quartz cuvette (Agilent QS, $l = 1 \text{ cm}$) containing ligand solution ($c_0 = 2 \times 10^{-5} \text{ mol dm}^{-3}$ to $3 \times 10^{-5} \text{ mol dm}^{-3}$) thermostatted at (25.0 ± 0.1) °C. Spectra were recorded at 2 nm data interval and an integration time of 0.4 s, and were processed by HypSpec program.^[67]

Microcalorimetric measurements were performed by an isothermal titration calorimeter Malvern Microcal VP-ITC at 25.0 °C. Titrations were conducted by automated stepwise addition of metal cation solution ($c_0 = 1 \times 10^{-3} \text{ mol dm}^{-3}$ to $9 \times 10^{-2} \text{ mol dm}^{-3}$) into the ligand solution ($c_0 = 7 \times 10^{-5} \text{ mol dm}^{-3}$ to $1 \times 10^{-4} \text{ mol dm}^{-3}$). Measured enthalpy changes were corrected for the heats of dilution of titrant in pure solvent. Non-linear least-square analyses of the calorimetric titration data were carried out by means of OriginPro 7.0 and OriginPro 7.5 programs.

¹H NMR titration experiments, as well as ¹H and ¹³C characterizations of the synthesized compounds, were conducted on Bruker Avance III HD 400 MHz/54 mm Ascend spectrometer equipped with 5 mm PA BBI 1H/D-BB probe with z-gradient and automatic tuning. All ¹H spectra were obtained using 64 K data points, spectral width of 20 ppm based on 16 scans, whereas ¹³C spectra were obtained using 64 K data points, spectral width of 220 ppm based on 4096 scans. Titrations were performed by stepwise addition of metal cation solution ($c_0 = 2 \times 10^{-2} \text{ mol dm}^{-3}$ to 0.2 mol dm^{-3}) into the ligand solution ($1 \times 10^{-3} \text{ mol dm}^{-3}$) in MeOD-*d*₃ with TMS as internal standard, thermostatted at 25 °C. Titration data were processed by HypNMR program.^[67]

IR spectroscopic analysis was conducted by PerkinElmer Spectrum Two spectrometer equipped with diamond UATR accessory. IR spectra were processed by Perkin Elmer Spectrum 10.4.2. program.^[68]

Molecular Dynamics Simulations

The molecular dynamics simulations were carried out by means of the GROMACS package (version 2018.6).^[69–74] Intramolecular and nonbonded intermolecular interactions were modelled by the CHARMM36 (Chemistry at HARvard Macromolecular Mechanics) force field.^[75] Partial charges of phenanthridine atoms were calculated for a model compound, namely 6-(phenoxyethyl)phenanthridine with CGENFF web server.^[76–78] The initial structure of the free

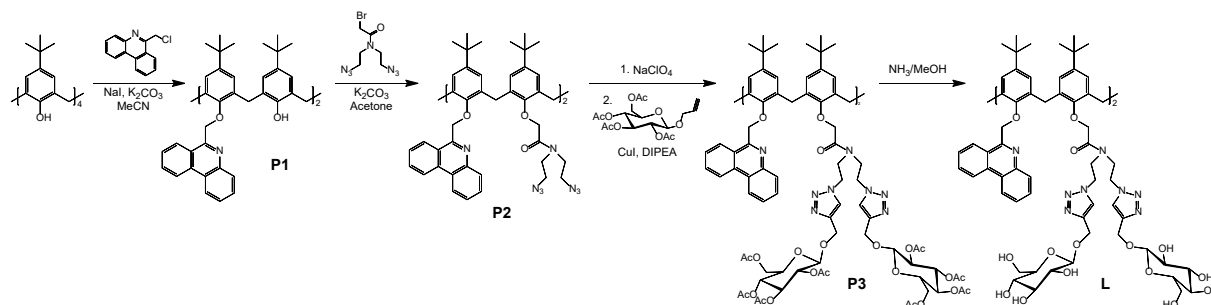
ligand was that in which the calixarene *basket* had a conformation of a flattened *cone*, whereas the initial structures of calixarene complexes were made by placing a cation between ether and carbonyl oxygen atoms of the lower-rim substituents. The L, ML⁺, and ML²⁺ species (M denotes alkali or alkaline earth metal) were solvated in a cubical box (edge length 60 Å) of methanol with periodic boundary conditions. The solvent boxes were equilibrated prior to solvation of the ligand and complexes. The solute concentration in such a box was about 0.01 mol dm⁻³. In all simulations an energy minimization procedure was performed followed by 50.5 ns of NpT production simulation, with the time constant of 1 ps. The first 0.5 ns of production simulation were discarded in the data analysis. The integrator used for the propagation and for the temperature control was stochastic dynamics algorithm^[79] with a time step of 1 fs. During simulation, the temperature and pressure were kept at 298 K and 1 bar, respectively. The cutoff radius for nonbonded van der Waals and short-range Coulomb interactions was 15 Å. Long-range Coulomb interactions were treated by the Ewald method as implemented in the PME (Particle Mesh Ewald) procedure.^[80] The representative molecular structures of L and its complexes were obtained by PCA (Principal Component Analysis) on coordination matrix whose rows contained cation-carbonyl oxygen atoms and cation-phenanthridine nitrogen atoms distances during simulation. Angles between metal cations and carbonyl groups were added to the coordination matrix as well. The chosen structures were closest to the centroids of the most populous clusters in space defined by the first two principal components. The coordination matrix of free ligand was assembled of distances of carbonyl oxygen and phenanthridine nitrogen atoms from geometric center of phenol oxygen atoms. The angles between this geometric center and carbonyl groups were also used. Figures of molecular structures were created using VMD software.^[81]

RESULTS AND DISCUSSION

Synthesis

The synthetic route to ligand L is shown in Scheme 1. The phenanthridine derivative P1 was obtained by the addition of 6-(chloromethyl)phenanthridine to *p*-*tert*-butylcalix[4]arene where the degree of functionalization was controlled by the molar ratio of reactants in the reaction mixture. The remaining distal positions were functionalized using *N,N*-bis(2-azidoethyl)-2-bromoacetamide to yield compound P2. The following *click* reaction with the glycosyl donor was performed on sodium complex of P2 which was obtained by the addition of sodium perchlorate prior to other reagents (in the absence of cation the decomposition of phenanthridine subunit occurred). After the *click*

reaction sodium and other metals were removed by extensive washing of DCM solution of **P3** with mQ water. The desired compound **L** was obtained by removing the acetyl protection groups on glucose subunits using NH_3/MeOH .



Scheme 1. Synthesis of calix[4]arene glycoconjugate **L**.

Complexation of Alkali Metal Cations

Upon addition of alkali metal cation solutions to that of **L** in methanol, significant changes in the ligand UV spectrum occurred, accompanied by the appearance of several neat isosbestic points. As an example, spectrophotometric titration of **L** with sodium perchlorate is shown in Figure 1, whereas the corresponding titrations with other alkali metal salts are presented in Figures S10, S16, and S18, Supporting Information. Stability constants determined by processing these data according to the model comprising formation of the complex of 1:1 stoichiometry are listed in Table 1. The UV spectrum of **L** mostly originates from the absorption of phenanthridine chromophore, which indicates the involvement of this moiety in the cation coordination.

Although certain changes in spectra could be seen during titration with cesium chloride (Figure S22, Supporting Information), they were insufficient for quantitative analysis, suggesting a very weak affinity of the ligand towards larger cesium cation.

Complexation of alkali metal cations was also followed by spectrofluorimetry (Figures 2, S13, S17, and S19, Supporting Information). In all cases the fluorescence of the phenanthridine group was enhanced by cation addition, which can be explained by the reduction of fluorescence quenching caused by photoinduced electron transfer (PET) in the free ligand compared to the complexed one.^[47] Stability constants obtained by analysis of spectrofluorimetric titrations data are given in Table 1 and are in good agreement with those determined by other methods. The exception is the equilibrium constant for the reaction of rubidium cation and **L** since in this case the fluorimetric data collected under the experimental conditions used could not be reliably analyzed.

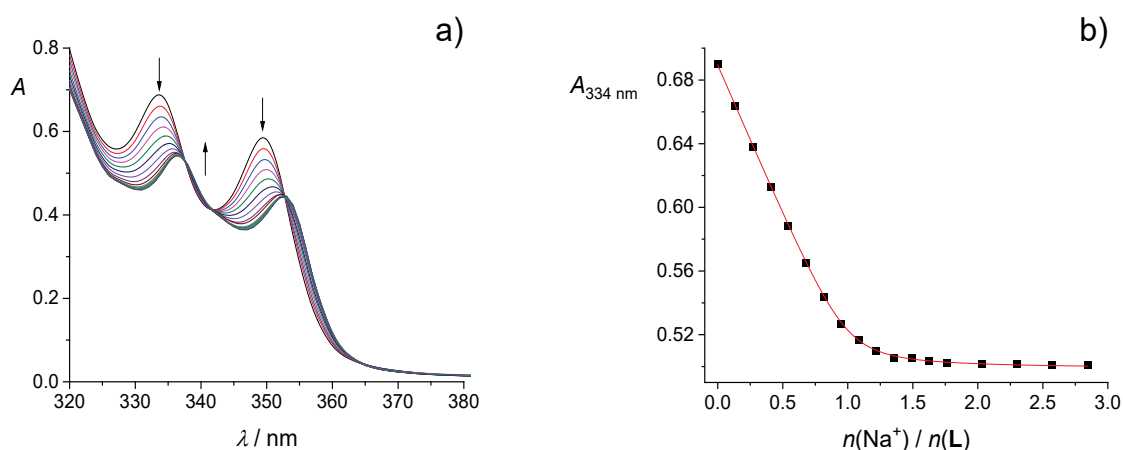


Figure 1. a) Spectrophotometric titration of **L** ($c_0 = 7.54 \times 10^{-5} \text{ mol dm}^{-3}$) with NaClO_4 ($c = 1.01 \times 10^{-3} \text{ mol dm}^{-3}$) in MeOH. $V_0 = 2.2 \text{ mL}$; $l = 1 \text{ cm}$. Spectra are corrected for dilution. b) Absorbance at 334 nm as a function of cation to **L** molar ratio. ■ experimental; — calculated.

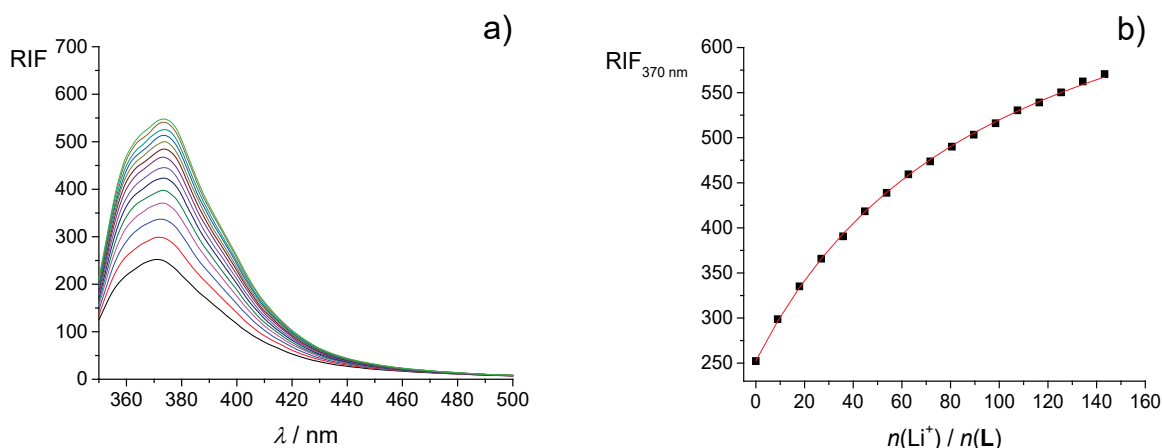


Figure 2. a) Spectrofluorimetric titration of **L** ($c_0 = 2.25 \times 10^{-5} \text{ mol dm}^{-3}$) with LiClO_4 ($c_0 = 2.02 \times 10^{-2} \text{ mol dm}^{-3}$) in MeOH. $V_0 = 2.5 \text{ mL}$; $\lambda_{\text{ex}} = 330 \text{ nm}$; excitation slit 10 nm ; emission slit 10 nm . Spectra are corrected for dilution. b) Relative intensity of fluorescence at 370 nm as a function of cation to **L** molar ratio. ■ experimental; – calculated.

Microcalorimetric titrations enabled determination of enthalpic and entropic contributions to the standard reaction Gibbs energies (derived from the corresponding complex stability constants). An example of such an experiment is presented in Figure 3 and the results of other titrations are shown in Figures S11, S14, and S20, Supporting Information.

As can be seen from the data given in Table 1, all reactions are enthalpy driven and entropically unfavorable, which is often the case with the complexation of alkali metal cations by calix[4]arene derivatives.^[6,37,40,62] The binding of Na^+ is by far the most exothermic resulting in the peak affinity for this cation. The complexation entropy is the least unfavorable for Li^+ binding, whereas the absolute value of complexation enthalpy is the lowest for this reaction. That is mainly due to the strongest solvation of Li^+ among the other

first-group cations.^[82,83] Namely, the cation desolvation, which takes place in the course of the complexation reaction, is in this case entropically the most advantageous ($\Delta_{\text{sol}}S^\circ(\text{M}^+) / \text{J K}^{-1} \text{ mol}^{-1} = -214 (\text{Li}^+), -212 (\text{Na}^+), -173 (\text{K}^+), -161 (\text{Rb}^+)$), but on the other hand energetically quite demanding ($\Delta_{\text{sol}}H^\circ / \text{kJ mol}^{-1} = -550 (\text{Li}^+), -439 (\text{Na}^+), -353 (\text{K}^+), -327 (\text{Rb}^+)$).^[83] From the cation solvation point of view, such an interplay between enthalpic and entropic contributions puts the K values of K^+ and Rb^+ complexes with **L** in between those with lithium and sodium cations (Table 1). However, when comparing stabilities of complexes in the same solvent, apart from cation solvation, that of the complex should also be considered. In this respect, the inclusion of solvent molecules into the calixarene hydrophobic cone plays an important role. This topic is discussed later in relation to the results of MD simulations.

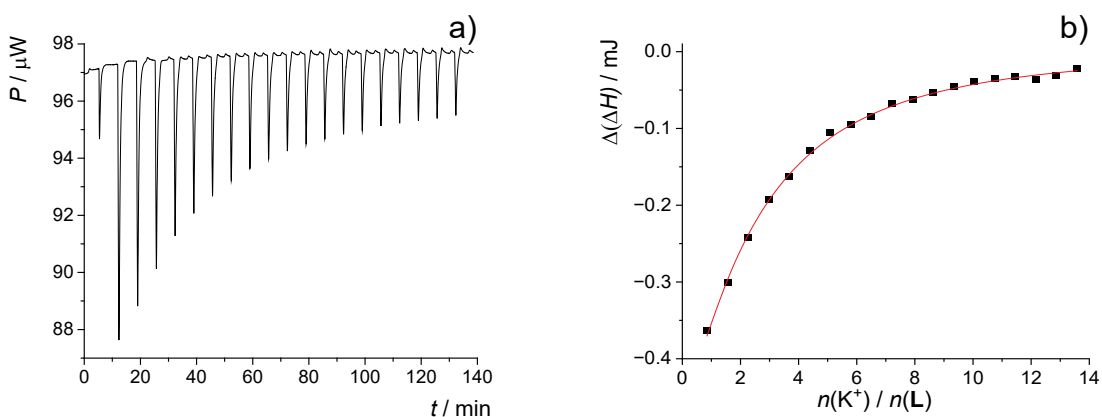


Figure 3. Microcalorimetric titration of **L** ($c_0 = 7.54 \times 10^{-5} \text{ mol dm}^{-3}$), $V = 1.43 \text{ cm}^3$) with KClO_4 ($c_0 = 5.09 \times 10^{-3} \text{ mol dm}^{-3}$) in MeOH at $25 \text{ }^\circ\text{C}$. a) Thermogram. b) Dependence of successive enthalpy changes on cation to **L** molar ratio. ■ experimental; – calculated.

Table 1. Thermodynamic parameters for formation of complexes of **L** with alkali metal cations in methanol at 25 °C. In the cases of repeated measurements, uncertainties are given in parentheses as standard errors of the mean ($N = 3$).

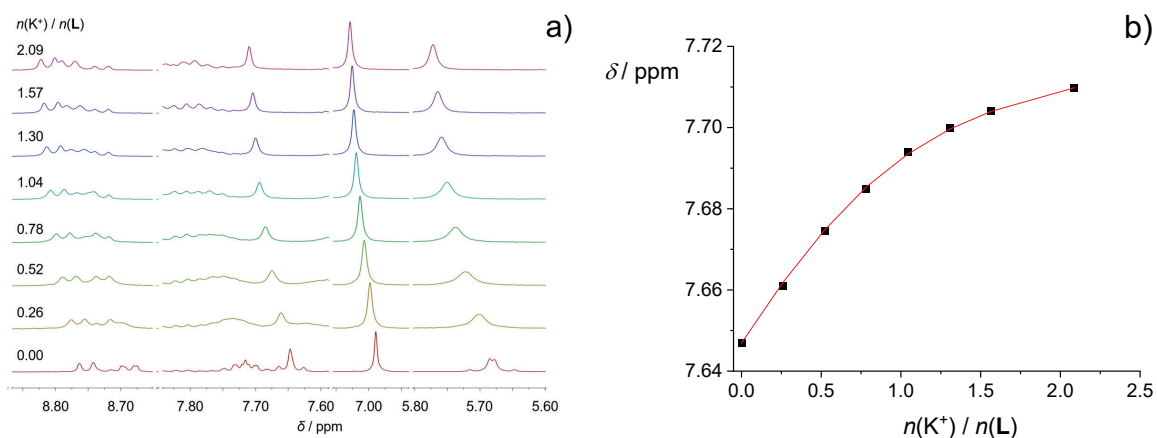
cation	$\log K(\text{ML}^+)$				$\frac{\Delta_r G^\circ}{\text{kJ mol}^{-1}}$ (d)	$\frac{\Delta_r H^\circ}{\text{kJ mol}^{-1}}$ (d)	$\frac{\Delta_r S^\circ}{\text{J K}^{-1} \text{ mol}^{-1}}$ (d)
	(a)	(b)	(c)	(d)			
Li ⁺	2.76(1)	2.61(3)	2.57	2.80(2)	-15.98(9)	-19.0(8)	-10(3)
Na ⁺	5.69(1)	5.66(2)	— ^(e)	5.65(1)	-32.25(6)	-41.9(7)	-32(2)
K ⁺	3.50(3)	3.28(2)	3.44	3.52(1)	-20.09(7)	-31(1)	-36(6)
Rb ⁺	2.33(1)	— ^(f)	2.27	2.28(3)	-13.0(2)	-31(2)	-59(6)

Determined by: (a) spectrophotometry, (b) spectrofluorimetry, (c) ¹H NMR, (d) microcalorimetry, (e) too high to be determined by NMR titration, (f) data could not be reliably processed.

The complex stability constants were also determined by ¹H NMR spectroscopy. In the case of sodium complexation, slow exchange on the NMR time scale was observed causing the appearance of the second set of signals in the NMR spectrum (Figure S15, Supporting Information), as opposed to the complexes of **L** with other alkali metal cations which exhibited fast exchange (Figures 4, S12, and S21, Supporting Information). Stability constant of the NaL⁺ complex was too large to be determined by NMR spectroscopy, whereas the equilibrium constants corresponding to Li⁺, K⁺, and Rb⁺ complexation by **L** calculated by processing ¹H NMR titration data agree well with those obtained by other techniques (Table 1).

It is interesting to compare stabilities of the complexes of the ligands which are structurally different to **L**, but contain the same substituent motifs, *i.e.* tertiary amides, triazole-glucose and phenanthridine moieties at the lower rim. Such comparison for alkali metal cation complexes in methanol as a solvent is presented in Figure 5. As expected for calix[4]arene derivatives, the most stable complexes are those with sodium cation. The number of tertiary-amide-based pendant arms is of considerable importance, whereby the attachment of triazole or triazole-

glucose motif to the amide nitrogen atom seems to slightly decrease the complex stability. The latter could be tentatively explained by considering steric hindrances in the cation-ligand complexes due to the presence of bulkier functional groups and their (de)solvation in the course of cation-binding process. The influence of the number of tertiary-amide carbonyl oxygen atoms in the cation-binding site is most pronounced for the Na⁺ complexation, less so for K⁺, and practically diminishes in the case of Li⁺. This could be explained as follows. Among alkali metal cations, sodium cation is by its size the most compatible with the calix[4]arene binding site comprised of four ether and four carbonyl oxygen atoms, often being coordinated by all ether oxygens and most of the carbonyl ones. Therefore, reducing the number of the latter considerably decreases Na⁺ interaction with the ligand, which is not so pronounced in the case of the larger K⁺ coordination. At the same time, in the case of phenanthridine-containing ligands, Na⁺ is only weakly coordinated by the nitrogen atom of this group. However, the interaction between potassium cation and nitrogen atoms of phenanthridine groups is stronger (see the results of MD simulations below and those described in ref. [50]) and partially compensates the “loss” of tertiary-

**Figure 4.** a) ¹H NMR titration of **L** ($c_0 = 1.42 \times 10^{-3} \text{ mol dm}^{-3}$) with KClO_4 ($c = 3.19 \times 10^{-2} \text{ mol dm}^{-3}$) in MeOD at 25 °C. b) Chemical shift of phenanthridine protons at 7.65 ppm as a function of cation to **L** molar ratio. ■ experimental; — calculated.

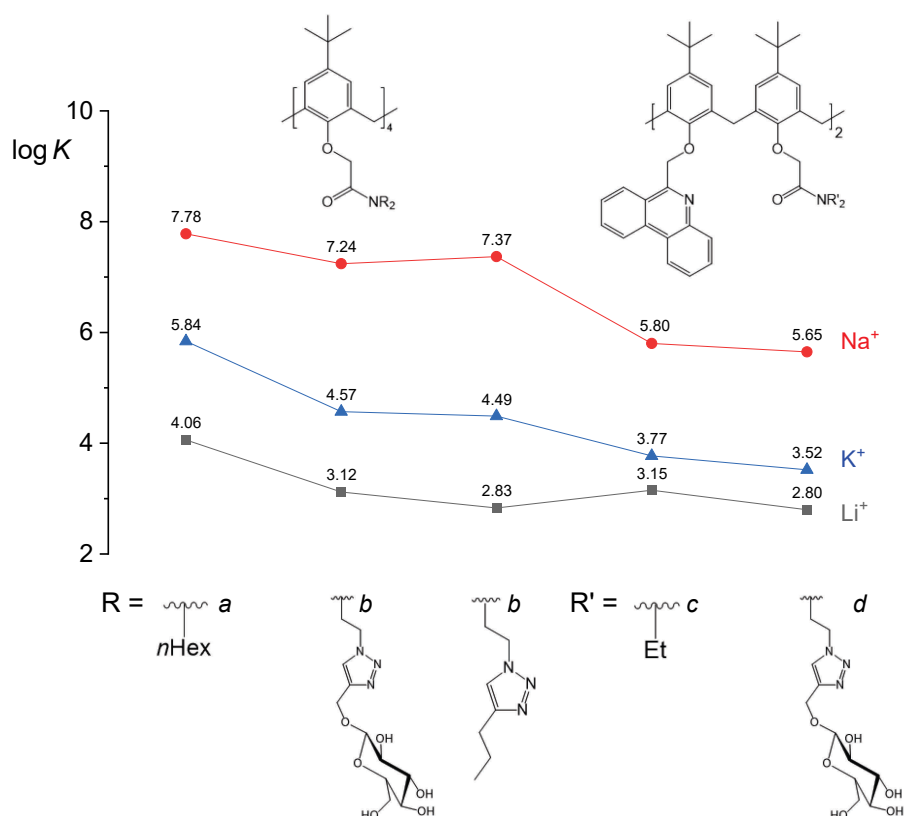


Figure 5. Comparison of thermodynamic stabilities of alkali metal cations complexes with calixarene derivatives comprising tertiary-amide, triazole-glucose, and phenanthridine moieties in methanol at 25 °C. Stability constants taken from: *a* ref. [52], *b* ref. [62], *c* ref. [50], *d* this work.

amide substituents. The smaller lithium cation realizes the interactions with the herein considered receptors *via* almost all ether oxygen atoms and to the less extent (compared to Na⁺ and K⁺) with carbonyl oxygens, whereas the interaction with phenanthridine nitrogen atoms is in the case of this cation almost completely absent (see later and refs. [47,50]). The overall effect of the established or missing interactions between the cations and ligand binding site is reflected in the complex stability constants given in Figure 5.

Complexation of Alkaline Earth Metal Cations

The binding affinities of **L** towards alkaline earth metal cations in methanol were also studied by means of spectrophotometric, fluorimetric, ¹H NMR, and calorimetric titrations. The results obtained spectrometrically are presented in Figures 6–8 and S23–S31, Supporting Information, and stability constants of the ML²⁺ complexes determined by the analyses of the corresponding data are listed in Table 2. Rather low stabilities of the complexes

required addition of large amounts of alkaline earth metal cation salts to reach significant percentage of complex formation. Consequently, titrant dilution heats were quite high and comparable to those resulted from the binding reactions, preventing in these cases the calorimetric determination of thermodynamic parameters of cations complexation. Although we do not have direct experimental evidence, the inconsistency between the equilibrium constants obtained spectrofluorimetrically and those measured by UV absorption and NMR spectroscopies can be tentatively explained by considering the possibility that the equilibrium constants determined by emission spectroscopy corresponds to the reaction of the ligand in its excited state.^[84,85]

Considering the cation charges, one would expect that **L** would be a better binder of alkaline earth metal cations compared to the alkali ones of the similar ionic radii. However, quite the opposite was observed (Tables 1 and 2). For example, crystallographic radius of Ca²⁺ for coordination number 6 is 1.00 Å and that of Na⁺ is 1.02 Å.^[86]

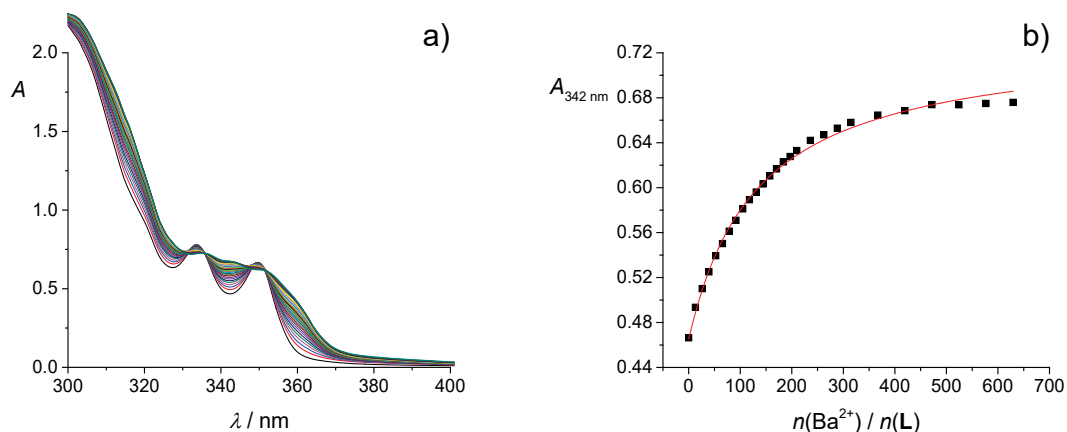


Figure 6. a) Spectrophotometric titration of **L** ($c_0 = 1.74 \times 10^{-4} \text{ mol dm}^{-3}$) with $\text{Ba}(\text{ClO}_4)_2$ ($c = 0.10 \text{ mol dm}^{-3}$) in MeOH. $V_0 = 2.2 \text{ mL}$; $l = 1 \text{ cm}$; $\vartheta = (25.0 \pm 0.1) \text{ }^\circ\text{C}$. Spectra are corrected for dilution. b) Absorbance at 342 nm as a function of cation to **L** molar ratio. ■ experimental; – calculated.

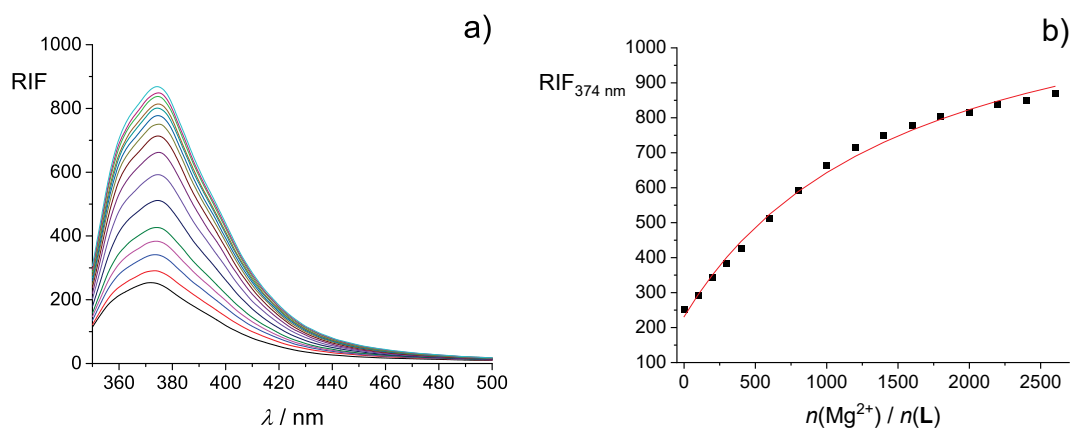


Figure 7. a) Fluorimetric titration of **L** ($c_0 = 3.41 \times 10^{-5} \text{ mol dm}^{-3}$) with $\text{Mg}(\text{ClO}_4)_2$ ($c = 0.15 \text{ mol dm}^{-3}$) in MeOH. $V_0 = 2.5 \text{ mL}$; $\vartheta = (25.0 \pm 0.1) \text{ }^\circ\text{C}$; $\lambda_{\text{ex}} = 330 \text{ nm}$; excitation slit 10 nm; emission slit 10 nm. Spectra are corrected for dilution. b) Relative intensity of fluorescence at 374 nm as a function of cation to **L** molar ratio. ■ experimental; – calculated.

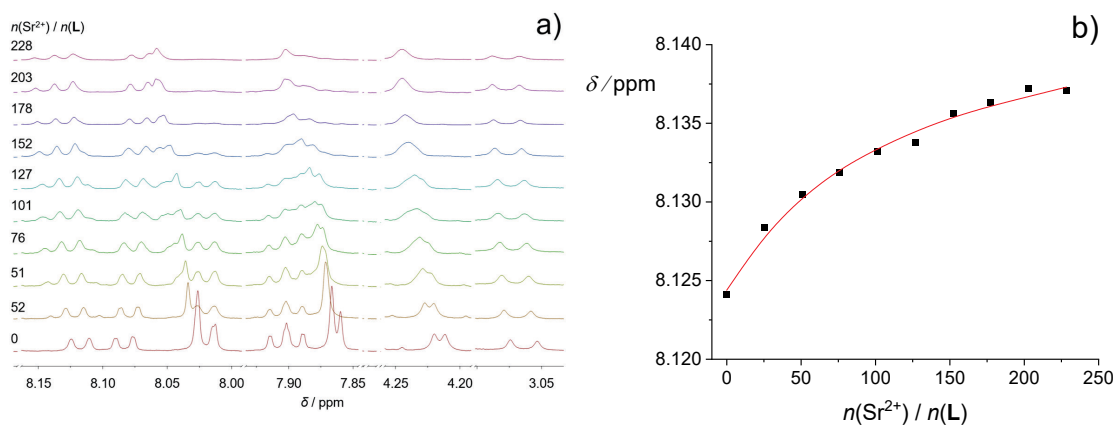


Figure 8. a) ^1H NMR titration of **L** ($c_0 = 1.57 \times 10^{-4} \text{ mol dm}^{-3}$) with $\text{Sr}(\text{ClO}_4)_2$ ($c = 9.98 \times 10^{-2} \text{ mol dm}^{-3}$) in MeOD. b) Chemical shift of phenanthridine protons at 8.12 ppm as a function of cation to **L** molar ratio. ■ experimental; – calculated.

Table 2. Stability constants of complexes of **L** with alkaline earth metal cations in methanol at 25 °C. In the cases of repeated measurements, uncertainties are given in parentheses as standard errors of the mean ($N = 3$).

cation	log $K(ML^{2+})$		
	(a)	(b)	(c)
Mg ²⁺	1.96(3)	1.09	2.13
Ca ²⁺	1.77(1)	0.55	1.12
Sr ²⁺	2.10(3)	1.81(1)	1.66
Ba ²⁺	1.60(1)	0.91	1.51

Determined by: (a) spectrophotometry, (b) spectrofluorimetry, (c) ¹H NMR

Despite this similarity and higher charge of calcium cation, stability constant of CaL²⁺ complex is much lower than that of NaL⁺. To explain this finding, one should primarily take into account the difference in solvation of the first- and second-group cations. As can be seen from the solvation thermodynamic parameters given in Table S4, Supporting Information, due to the higher charge density (*i.e.* q/r ratio), the latter are considerably better solvated in methanol than the former. That makes the cation desolvation, taking place in the course of complexation reaction, more unfavorable for alkaline earth metal cations, and this is the main reason behind the observed lower stability of the ML²⁺ relative to ML⁺ complexes in methanol.

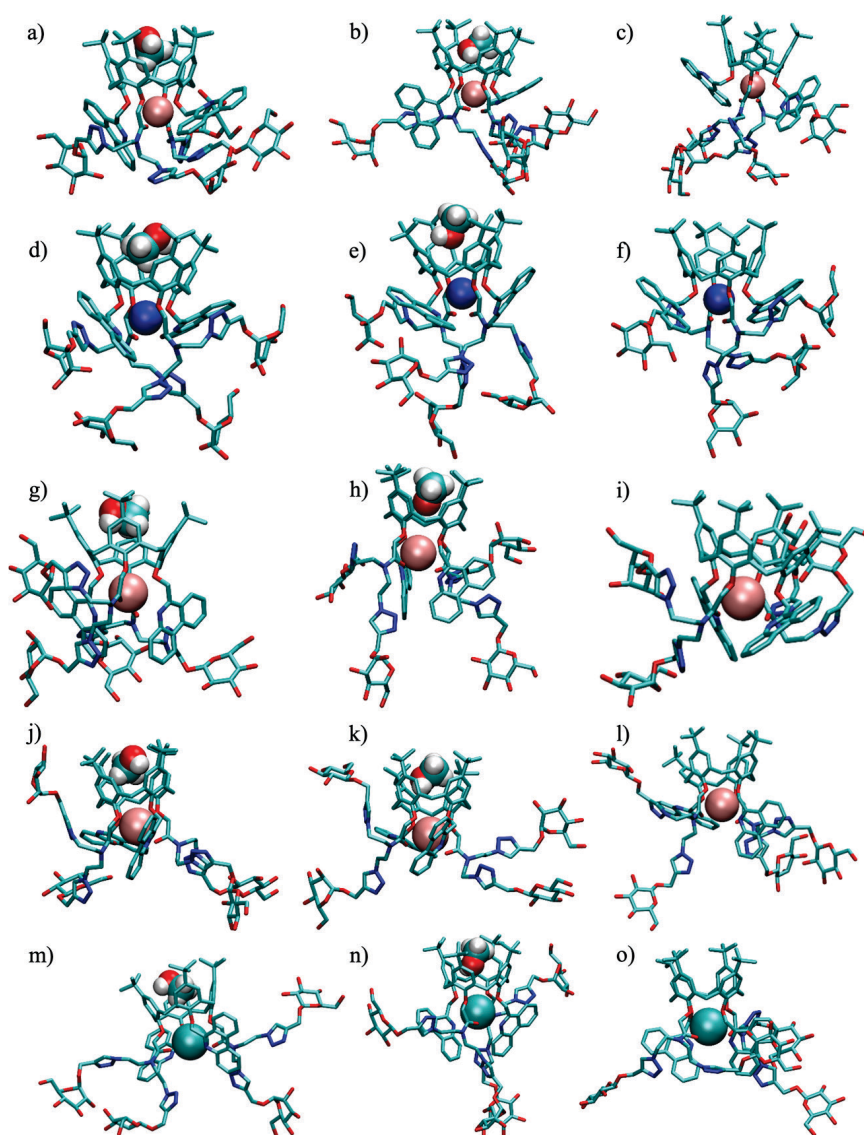


Figure 9. Representative structures of a) LiLMeOH⁺, b) LiLMeOH⁺, c) LiL⁺, d) NaLMeOH⁺, e) NaLMeOH⁺, f) NaL⁺, g) KLMeOH⁺, h) KLMeOH⁺, i) KL⁺, j) RbLMeOH⁺, k) RbLMeOH⁺, l) RbL⁺, m) CsLMeOH⁺, n) CsLMeOH⁺, and o) CsL⁺ adducts obtained by MD simulations at 25 °C. Hydrogen atoms of **L** are omitted for clarity.

Molecular Dynamics Simulations

The classical molecular dynamics simulations of **L** and its alkali and alkaline earth metal complexes in methanol were carried out to get an insight into their structures and the solvent molecule inclusion into the calixarene hydrophobic *basket*.

The results of MD simulations of free **L** are given in the Supporting Information (Table S1 and Figure S32 and S33). During most of the simulation time (91.5 %), the ligand was present in the form of **LMeOH** adduct in which methanol molecule was included in the calixarene *basket* with methyl group pointing inwards (Figure S33a, Supporting Information). During that time, 5 solvent molecules exchanged in the calixarene cavity. The differences between distances of the opposite aryl carbon atoms connected to the *tert*-butyl groups at the calixarene upper rim (Table S1, Supporting Information) of the free ligand and its methanol adduct indicated that calixarene *basket* of free **L** had flattened *cone* shape of C_2 symmetry (the distances differ significantly), whereas in the adduct conformation changed to almost regular *cone* of approximately C_4 symmetry (the distances nearly the same).

In the simulations of **L** complexes with alkali metal cations (Figure 9 and S34, Table S2, Supporting Information), besides species without solvent molecule included (Figure 9c, f, i, l, and o), two types of methanol adducts were noticed: the much more predominant one (78–98 % of the simulation time) with methyl group pointing to metal ion (**MLMeOH**⁺, Figure 9a, d, g, j, and m) and another, denoted as **MLMeOH**['], in which hydroxyl group was oriented towards the cation (Figure 5b, e, h, k, and n). In all cases, cation was on average coordinated with almost all ether and carbonyl oxygen atoms. The average number of coordinating phenanthridine nitrogen atoms increased with the cation size, being 0 (Li⁺, Na⁺), 0.66 (K⁺), 0.9 (Rb⁺), and 1.34 (Cs⁺). A rather weak coordination by triazole group was also observed, but only in the case of complexes with larger potassium, rubidium, and cesium cations (Table S2, Supporting Information). The differences in distances of the opposite aryl carbon atoms connected to the *tert*-butyl groups were larger in the **MLMeOH**⁺ adducts comprising larger cations, which indicated higher flexibility of calixarene *basket* in these species (Table S2, Supporting Information).

The results of simulations and the obtained representative structures of alkaline earth metal cation complexes are presented in Figure 10 and S39, Table S3, Supporting Information. Interestingly, magnesium and calcium complexes were found to be predominantly in **MLMeOH**^{2+'} form (cation coordinated by hydroxyl oxygen atom of the included methanol molecule), whereas complexes without included solvent molecule were not

detected. Along with the fact that no exchange of MeOH molecules inside the *basket* was observed, this clearly indicated stronger inclusion of the solvent molecule and its cation coordination in **MgLMeOH**^{2+'} and **CaLMeOH**^{2+'} adducts compared to alkali metal and other alkaline earth metal cations complexes (Tables S2 and S3, Supporting Information). Strontium and barium complexes were found to exist as all three types of species (with and without MeOH included), with the adduct in which methanol methyl group was facing the cation being the most abundant. The above findings can be rationalized by considering the size and charge of metal ions. As expected, the smaller size and higher charge of cation favor its coordination by included solvent molecule, *i.e.* formation of **MLMeOH**^{2+'} species. Regarding the coordination of alkaline earth metal cations by the atoms forming the **L** binding site, it was found that the average number of ether and carbonyl oxygen atoms decreased with ion size, whereas, as in the case of first-group cations, the opposite was observed for coordination with phenanthridine and triazole nitrogen atoms (Table S3, Supporting Information).

CONCLUSION

The calix[4]arene derivative **L** was designed and synthesized as a compound comprising highly efficient cation-binding groups (tertiary amides), phenanthridine moieties to ensure its fluorescence, and glucose functionalities to increase its solubility in polar solvents. The complexation of alkali and alkaline earth metal cations by this ligand in methanol was comprehensively studied by several experimental methods and molecular dynamics simulations. The determined thermodynamic reaction parameters showed that the complexation of **L** with alkali metal cations was in all cases enthalpy driven and entropically unfavorable. The ligand was proven to be significantly less effective in binding the second- compared to the first-group cations in methanol, which was primarily ascribed to the rather large difference in the cation solvation in this solvent. Computational investigations provided an insight into the structures of **L** and its complexes and showed that, depending on the cation size and charge, the receptor binding site consisted of various numbers of ether and carbonyl oxygen atoms. In the case of larger cations, phenanthridine nitrogen atoms were involved in the cation coordination as well. It was also observed that during almost all the simulation time the hydrophobic cavity of the free and complexed ligand was occupied by methanol molecule. The solvent molecule was, depending on the cation charge to radius ratio, oriented either with methyl group pointing to cation or oppositely, with OH group facing the metal ion (this orientation was favored in the case of higher charge density cations).

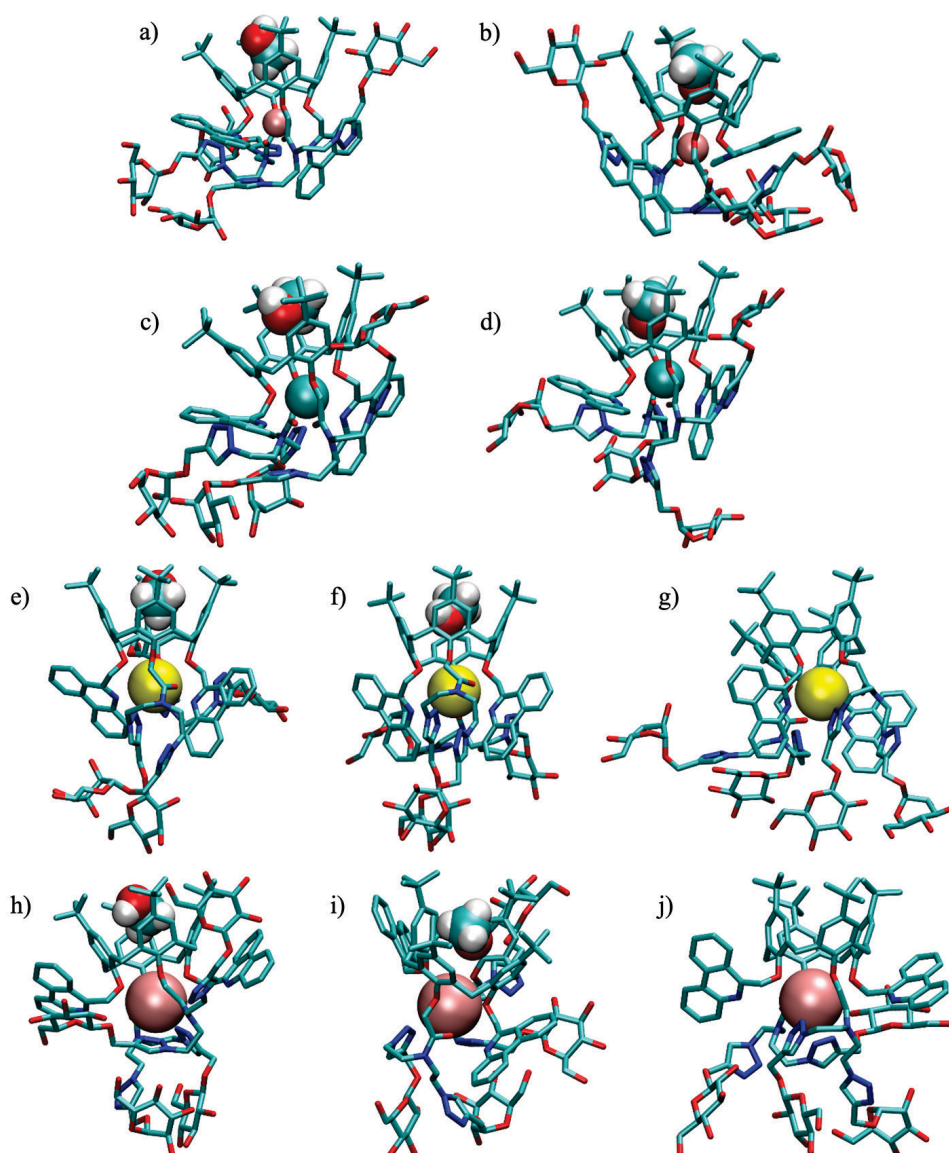


Figure 10. Representative structures of a) MgLMeOH^{2+} , b) $\text{MgLMeOH}^{\prime 2+}$, c) CaLMeOH^{2+} , d) $\text{CaLMeOH}^{\prime 2+}$, e) SrLMeOH^{2+} , f) $\text{SrLMeOH}^{\prime 2+}$, g) SrL^{2+} , h) BaLMeOH^{2+} , i) $\text{BaLMeOH}^{\prime 2+}$, and j) BaL^{2+} adducts obtained by MD simulations at 25 °C. Hydrogen atoms of **L** are omitted for clarity.

The solvation effects and the size compatibility of the cation and calix[4]arene binding site make **L** rather selective for sodium with respect to other cations in methanol. According to the data listed in Tables 1 and 2, the selectivity towards Na^+ , expressed as the ratio of the stability constants of the corresponding complexes, amounts to >100 regarding K^+ , ≈ 1000 for Li^+ , and >2500 for all other cations.

Although the aqueous solubility of **L** was found to be lower than predicted, it can be envisaged that this compound can serve as a template for design and synthesis of other neutral and fluorescent water-soluble calixarene-based cation receptors.

Acknowledgment. This work was funded by the European Union – NextGenerationEU project ToSiAn (Total synthesis of bioactive metabolites - From deep sea microorganisms to new class of antibiotics and synthetic methodologies, NPOO.C3.2.R2-I1.06.00430).

Supplementary Information. Supporting information to the paper is attached to the electronic version of the article at: <https://doi.org/10.5562/cca4115>.

PDF files with attached documents are best viewed with Adobe Acrobat Reader which is free and can be downloaded from [Adobe's web site](https://www.adobe.com/acrobat).

REFERENCES

- [1] Z. Asfari, *Calixarenes 2001*, Kluwer Academic Publishers, Dordrecht, **2001**.
<https://doi.org/10.1007/0-306-47522-7>
- [2] C. D. Gutsche, *Calixarenes Revisited*, Royal Society Of Chemistry, **2007**.
- [3] C. D. Gutsche, *Calixarenes: An Introduction*, RSC Publishing, Cambridge, **2008**.
- [4] L. Baldini, F. Sansone, A. Casnati, R. Ungaro, in *Supramolecular Chemistry* (Eds.: P.A. Gale, J.W. Steed), Wiley, **2012**.
- [5] P. Neri, J. L. Sessler, M.-X. Wang, Eds., *Calixarenes and Beyond*, Springer International Publishing, Cham, **2016**.
<https://doi.org/10.1007/978-3-319-31867-7>
- [6] A. F. Danil de Namor, R. M. Cleverley, M. L. Zapata-Ormachea, *Chem. Rev.* **1998**, *98*, 2495–2526.
<https://doi.org/10.1021/cr970095w>
- [7] D. M. Homden, C. Redshaw, *Chem. Rev.* **2008**, *108*, 5086–5130. <https://doi.org/10.1021/cr8002196>
- [8] G. Sachdeva, D. Vaya, C. M. Srivastava, A. Kumar, V. Rawat, M. Singh, M. Verma, P. Rawat, G. K. Rao, *Coord. Chem. Rev.* **2022**, *472*, 214791.
<https://doi.org/10.1016/j.ccr.2022.214791>
- [9] F. Arnaud-Neu, G. Barrett, S. Fanni, D. Marrs, W. McGregor, M. A. McKervey, M.-J. Schwing-Weill, V. Vetrogon, S. Wechsler, *J. Chem. Soc., Perkin Trans. 2* **1995**, 453.
<https://doi.org/10.1039/p29950000453>
- [10] B. S. Creaven, D. F. Donlon, J. McGinley, *Coord. Chem. Rev.* **2009**, *253*, 893–962.
<https://doi.org/10.1016/j.ccr.2008.06.008>
- [11] S. N. Podyachev, N. E. Kashapova, V. V. Syakaev, S. N. Sudakova, R. R. Zainullina, M. Gruner, W. D. Habicher, T. A. Barsukova, F. Yang, A. I. Konovalov, *J. Incl. Phenom. Macrocycl. Chem.* **2014**, *78*, 371–380.
<https://doi.org/10.1007/s10847-013-0307-0>
- [12] I. Sviben, N. Galić, V. Tomišić, L. Frkanec, *New J. Chem.* **2015**, *39*, 6099–6107.
<https://doi.org/10.1039/C5NJ00805K>
- [13] W. B. Aparicio-Aragon, T. D. Ramos, A. F. D. D. Namor, *ACES* **2021**, *11*, 165–179.
<https://doi.org/10.4236/aces.2021.112011>
- [14] N. Basílio, L. Garcia-Rio, M. Martín-Pastor, *Langmuir* **2012**, *28*, 2404–2414.
<https://doi.org/10.1021/la204004h>
- [15] N. Basilio, B. Gómez, L. Garcia-Rio, V. Francisco, *Chemistry – A European Journal* **2013**, *19*, 4570–4576. <https://doi.org/10.1002/chem.201203377>
- [16] R. El Nashar, H. A. Wagdy, H. Aboul-Enein, *Curr. Anal. Chem.* **2009**, *5*, 249–270.
<https://doi.org/10.2174/157341109788680273>
- [17] G. A. Evtugyn, E. E. Stoikova, R. V. Shamagsumova, *Russ. Chem. Rev.* **2011**, *79*, 1071–1097.
<https://doi.org/10.1070/RC2010v079n12ABEH004107>
- [18] J. S. Kim, D. T. Quang, *Chem. Rev.* **2007**, *107*, 3780–3799. <https://doi.org/10.1021/cr068046j>
- [19] C. Rémy, H. Guyon, J.-N. Rebilly, I. Leray, O. Reinaud, *Chem. Eur. J.* **2017**, *23*, 8669–8677.
<https://doi.org/10.1002/chem.201700640>
- [20] R. Kumar, A. Sharma, H. Singh, P. Suating, H. S. Kim, K. Sunwoo, I. Shim, B. C. Gibb, J. S. Kim, *Chem. Rev.* **2019**, *119*, 9657–9721.
<https://doi.org/10.1021/acs.chemrev.8b00605>
- [21] T. L. Mako, J. M. Racicot, M. Levine, *Chem. Rev.* **2019**, *119*, 322–477.
<https://doi.org/10.1021/acs.chemrev.8b00260>
- [22] I. Krošl, E. Otković, I. Nikšić-Franjić, B. Colasson, O. Reinaud, A. Višnjevac, I. Piantanida, *New J. Chem.* **2022**, *46*, 6860–6869.
<https://doi.org/10.1039/D2NJ00061J>
- [23] H. Bakirci, A. L. Koner, M. H. Dickman, U. Kortz, W. M. Nau, *Angew. Chem. Int. Ed.* **2006**, *45*, 7400–7404.
<https://doi.org/10.1002/anie.200602999>
- [24] D. T. Schühle, J. A. Peters, J. Schatz, *Coord. Chem. Rev.* **2011**, *255*, 2727–2745.
<https://doi.org/10.1016/j.ccr.2011.04.005>
- [25] S. B. Nimse, T. Kim, *Chem. Soc. Rev.* **2013**, *42*, 366–386. <https://doi.org/10.1039/C2CS35233H>
- [26] J.-N. Rebilly, B. Colasson, O. Bistri, D. Over, O. Reinaud, *Chem. Soc. Rev.* **2015**, *44*, 467–489.
<https://doi.org/10.1039/C4CS00211C>
- [27] Y. Pan, X. Hu, D. Guo, *Angew. Chem. Int. Ed.* **2021**, *60*, 2768–2794.
<https://doi.org/10.1002/anie.201916380>
- [28] J. N. Martins, B. Raimundo, A. Rioboo, Y. Folgar-Cameán, J. Montenegro, N. Basílio, *J. Am. Chem. Soc.* **2023**, *145*, 13126–13133.
<https://doi.org/10.1021/jacs.3c01829>
- [29] A.-N. Lazar, F. Perret, M. Perez-Lloret, M. Michaud, A. W. Coleman, *Eur. J. Med. Chem.* **2024**, *264*, 115994.
<https://doi.org/10.1016/j.ejmech.2023.115994>
- [30] M. J. Webber, R. Langer, *Chem. Soc. Rev.* **2017**, *46*, 6600–6620. <https://doi.org/10.1039/C7CS00391A>
- [31] C. Gaeta, P. La Manna, M. De Rosa, A. Soriente, C. Talotta, P. Neri, *ChemCatChem* **2021**, *13*, 1638–1658. <https://doi.org/10.1002/cctc.202001570>
- [32] J. De Mendoza, F. Cuevas, P. Prados, E. S. Meadows, G. W. Gokel, *Angew. Chem. Int. Ed.* **1998**, *37*, 1534–1537. [https://doi.org/10.1002/\(SICI\)1521-3773\(19980619\)37:11%3C1534::AID-ANIE1534%3E3.3.CO;2-2](https://doi.org/10.1002/(SICI)1521-3773(19980619)37:11%3C1534::AID-ANIE1534%3E3.3.CO;2-2)
- [33] V. Sidorov, F. W. Kotch, G. Abdrakhmanova, R. Mizani, J. C. Fettingner, J. T. Davis, *J. Am. Chem. Soc.* **2002**, *124*, 2267–2278.
<https://doi.org/10.1021/ja012338e>

- [34] A. F. Danil de Namor, D. Kowalska, E. E. Castellano, O. E. Piro, F. J. Sueros Velarde, J. Villanueva Salas, *Phys. Chem. Chem. Phys.* **2001**, *3*, 4010–4021. <https://doi.org/10.1039/b104355m>
- [35] W. Śliwa, *J. Incl. Phenom. Macrocycl. Chem.* **2005**, *52*, 13–37. <https://doi.org/10.1007/s10847-005-0083-6>
- [36] W. Śliwa, T. Girek, *J. Incl. Phenom. Macrocycl. Chem.* **2010**, *66*, 15–41. <https://doi.org/10.1007/s10847-009-9678-7>
- [37] G. Horvat, V. Stilinović, T. Hrenar, B. Kaitner, L. Frkanec, V. Tomišić, *Inorg. Chem.* **2012**, *51*, 6264–6278. <https://doi.org/10.1021/ic300474s>
- [38] A. F. Danil de Namor, T. T. Matsufuji-Yasuda, K. Zegarra-Fernandez, O. A. Webb, A. El Gamouz, *Croat. Chem. Acta* **2013**, *86*, 1–19. <https://doi.org/10.5562/cca2170>
- [39] G. Horvat, V. Stilinović, B. Kaitner, L. Frkanec, V. Tomišić, *Inorg. Chem.* **2013**, *52*, 12702–12712. <https://doi.org/10.1021/ic4019184>
- [40] J. Požar, I. Nikšić-Franjić, M. Cvetnić, K. Leko, N. Cindro, K. Pičuljan, I. Borilović, L. Frkanec, V. Tomišić, *J. Phys. Chem. B* **2017**, *121*, 8539–8550. <https://doi.org/10.1021/acs.jpbc.7b05093>
- [41] E. Nomura, M. Takagaki, C. Nakaoka, M. Uchida, H. Taniguchi, *J. Org. Chem.* **1999**, *64*, 3151–3156. <https://doi.org/10.1021/jo982251k>
- [42] L. Frkanec, A. Višnjec, B. Kojić-Prodić, M. Žinić, *Chem. Eur. J.* **2000**, *6*, 442–453. [https://doi.org/10.1002/\(SICI\)1521-3765\(20000204\)6:3%3C442::AID-CHEM442%3E3.0.CO;2-1](https://doi.org/10.1002/(SICI)1521-3765(20000204)6:3%3C442::AID-CHEM442%3E3.0.CO;2-1)
- [43] V. Tomišić, N. Galić, B. Bertoša, L. Frkanec, V. Simeon, M. Žinić, *J. Incl. Phenom. Macrocycl. Chem.* **2005**, *53*, 263–268. <https://doi.org/10.1007/s10847-005-2024-9>
- [44] J. Požar, T. Preočanin, L. Frkanec, V. Tomišić, *J. Solution Chem.* **2010**, *39*, 835–848. <https://doi.org/10.1007/s10953-010-9550-9>
- [45] H. Ren, H. Wang, W. Wen, S. Li, N. Li, F. Huo, C. Yin, *Chem. Commun.* **2023**, *59*, 13790–13799. <https://doi.org/10.1039/D3CC04179D>
- [46] N. Galić, N. Burić, R. Tomaš, L. Frkanec, V. Tomišić, *Supramol. Chem.* **2011**, *23*, 389–397. <https://doi.org/10.1080/10610278.2010.521832>
- [47] M. Tranfić Bakić, D. Jadreško, T. Hrenar, G. Horvat, J. Požar, N. Galić, V. Sokol, R. Tomaš, S. Alihodžić, M. Žinić, L. Frkanec, V. Tomišić, *RSC Adv.* **2015**, *5*, 23900–23914. <https://doi.org/10.1039/C5RA01905B>
- [48] N. Bregović, N. Cindro, L. Frkanec, V. Tomišić, *Supramol. Chem.* **2016**, *28*, 608–615. <https://doi.org/10.1080/10610278.2016.1154147>
- [49] M. Tranfić Bakić, K. Leko, N. Cindro, T. Portada, T. Hrenar, L. Frkanec, G. Horvat, J. Požar, V. Tomišić, *Croat. Chem. Acta* **2017**, *90*, 711–725. <https://doi.org/10.5562/cca3308>
- [50] K. Leko, A. Usenik, N. Cindro, M. Modrušan, J. Požar, G. Horvat, V. Stilinović, T. Hrenar, V. Tomišić, *ACS Omega* **2023**, *8*, 43074–43087. <https://doi.org/10.1021/acsomega.3c06509>
- [51] A. F. Danil de Namor, S. Chahine, D. Kowalska, E. E. Castellano, O. E. Piro, *J. Am. Chem. Soc.* **2002**, *124*, 12824–12836. <https://doi.org/10.1021/ja020764+>
- [52] G. Horvat, L. Frkanec, N. Cindro, V. Tomišić, *Phys. Chem. Chem. Phys.* **2017**, *19*, 24316–24329. <https://doi.org/10.1039/C7CP03920D>
- [53] A. F. Danil de Namor, S. Chahine, E. E. Castellano, O. E. Piro, *J. Phys. Chem. A* **2005**, *109*, 6743–6751. <https://doi.org/10.1021/jp0514067>
- [54] A. S. de Araujo, O. E. Piro, E. E. Castellano, A. F. Danil de Namor, *J. Phys. Chem. A* **2008**, *112*, 11885–11894. <https://doi.org/10.1021/jp804198c>
- [55] A. F. Danil de Namor, N. A. De Sueros, M. A. McKervey, G. Barrett, F. A. Neu, M. J. Schwing-Weill, *J. Chem. Soc., Chem. Commun.* **1991**, 1546. <https://doi.org/10.1039/c39910001546>
- [56] N. Basilio, L. García-Río, M. Martín-Pastor, *J. Phys. Chem. B* **2010**, *114*, 7201–7206. <https://doi.org/10.1021/jp101474a>
- [57] V. Francisco, A. Piñeiro, W. M. Nau, L. García-Río, *Chem. Eur. J.* **2013**, *19*, 17809–17820. <https://doi.org/10.1002/chem.201302365>
- [58] D.-S. Guo, Y. Liu, *Acc. Chem. Res.* **2014**, *47*, 1925–1934. <https://doi.org/10.1021/ar500009g>
- [59] K. Wang, E.-C. Yang, X.-J. Zhao, Y. Liu, *RSC Adv.* **2015**, *5*, 2640–2646. <https://doi.org/10.1039/C4RA15047C>
- [60] K. Araki, A. Yanagi, S. Shinkai, *Tetrahedron* **1993**, *49*, 6763–6772. [https://doi.org/10.1016/S0040-4020\(01\)80420-8](https://doi.org/10.1016/S0040-4020(01)80420-8)
- [61] N. Cindro, J. Požar, D. Barišić, N. Bregović, K. Pičuljan, R. Tomaš, L. Frkanec, V. Tomišić, *Org. Biomol. Chem.* **2018**, *16*, 904–912. <https://doi.org/10.1039/C7OB02955A>
- [62] J. Požar, M. Cvetnić, A. Usenik, N. Cindro, G. Horvat, K. Leko, M. Modrušan, V. Tomišić, *Molecules* **2022**, *27*, 470. <https://doi.org/10.3390/molecules27020470>
- [63] L. Raszeja, A. Maghnooui, S. Hahn, N. Metzler-Nolte, *ChemBioChem* **2011**, *12*, 371–376. <https://doi.org/10.1002/cbic.201000576>
- [64] N. Cindro, Synthesis and complexation properties of calix[4]arene glycoconjugates, Doctoral Thesis, University of Zagreb, **2017**.

- [65] L. D. Pedro-Hernández, M. Martínez-García, *COC* **2022**, *26*, 71–80. <https://doi.org/10.2174/1385272825666211130164548>
- [66] T. K. Lindhorst, *Essentials of Carbohydrate Chemistry and Biochemistry*, Wiley-VCH, Weinheim, **2003**.
- [67] P. Gans, A. Sabatini, A. Vacca, *Talanta* **1996**, *43*, 1739–1753. [https://doi.org/10.1016/0039-9140\(96\)01958-3](https://doi.org/10.1016/0039-9140(96)01958-3)
- [68] Perkin Elmer Spectrum 10.4.2., Perkin Elmer Ltd., Waltham, Massachusetts, USA.
- [69] H. J. C. Berendsen, D. Van Der Spoel, R. Van Drunen, *Comput. Phys. Commun.* **1995**, *91*, 43–56. [https://doi.org/10.1016/0010-4655\(95\)00042-E](https://doi.org/10.1016/0010-4655(95)00042-E)
- [70] E. Lindahl, B. Hess, D. Van Der Spoel, *J. Mol. Model.* **2001**, *7*, 306–317. <https://doi.org/10.1007/s008940100045>
- [71] D. Van Der Spoel, E. Lindahl, B. Hess, G. Groenhof, A. E. Mark, H. J. C. Berendsen, *J. Comput. Chem.* **2005**, *26*, 1701–1718. <https://doi.org/10.1002/jcc.20291>
- [72] B. Hess, C. Kutzner, D. Van Der Spoel, E. Lindahl, *J. Chem. Theory Comput.* **2008**, *4*, 435–447. <https://doi.org/10.1021/ct700301q>
- [73] S. Pronk, S. Páll, R. Schulz, P. Larsson, P. Bjelkmar, R. Apostolov, M. R. Shirts, J. C. Smith, P. M. Kasson, D. Van Der Spoel, B. Hess, E. Lindahl, *Bioinformatics* **2013**, *29*, 845–854. <https://doi.org/10.1093/bioinformatics/btt055>
- [74] M. J. Abraham, T. Murtola, R. Schulz, S. Páll, J. C. Smith, B. Hess, E. Lindahl, *SoftwareX* **2015**, *1–2*, 19–25.
- [75] R. B. Best, X. Zhu, J. Shim, P. E. M. Lopes, J. Mittal, M. Feig, A. D. MacKerell, *J. Chem. Theory Comput.* **2012**, *8*, 3257–3273. <https://doi.org/10.1021/ct300400x>
- [76] A.-R. Allouche, *J. Comput. Chem.* **2011**, *32*, 174–182. <https://doi.org/10.1002/jcc.21600>
- [77] K. Vanommeslaeghe, A. D. MacKerell, *J. Chem. Inf. Model.* **2012**, *52*, 3144–3154. <https://doi.org/10.1021/ci300363c>
- [78] W. Yu, X. He, K. Vanommeslaeghe, A. D. MacKerell, *J. Comput. Chem.* **2012**, *33*, 2451–2468. <https://doi.org/10.1002/jcc.23067>
- [79] N. Goga, A. J. Rzepiela, A. H. De Vries, S. J. Marrink, H. J. C. Berendsen, *J. Chem. Theory Comput.* **2012**, *8*, 3637–3649. <https://doi.org/10.1021/ct3000876>
- [80] T. Darden, D. York, L. Pedersen, *J. Chem. Phys.* **1993**, *98*, 10089–10092. <https://doi.org/10.1063/1.464397>
- [81] W. Humphrey, A. Dalke, K. Schulten, *J. Mol. Graph. Model.* **1996**, *14*, 33–38. [https://doi.org/10.1016/0263-7855\(96\)00018-5](https://doi.org/10.1016/0263-7855(96)00018-5)
- [82] Y. Marcus, *Ion Properties*, Dekker, New York Basel, **1997**.
- [83] Y. Marcus, *Ions in Solution and Their Solvation*, Wiley, **2015**. <https://doi.org/10.1002/9781118892336>
- [84] J. F. Ireland, P. A. H. Wyatt, in *Advances in Physical Organic Chemistry*, Elsevier, **1976**, pp. 131–221. [https://doi.org/10.1016/S0065-3160\(08\)60331-7](https://doi.org/10.1016/S0065-3160(08)60331-7)
- [85] B. D. Wagner, *Phys. Chem. Chem. Phys.* **2012**, *14*, 8825. <https://doi.org/10.1039/c2cp40310b>
- [86] W. M. Haynes, *CRC Handbook of Chemistry and Physics*, CRC Press, Hoboken, **2014**, pp. 11–12. <https://doi.org/10.1201/b17118>